Analysis of IfE-Robot based Group Delay Variations for the Positioning and Navigation of Mobile Platforms

Tobias Kersten and Steffen Schön

Institut für Erdmessung (IfE)

Leibniz Universität Hannover

Schneiderberg 50, D-30167 Hannover, Germany

mail: kersten@ife.uni-hannover.de, schoen@ife.uni-hannover.de

***Abstract*—This contribution demonstrates the analysis and application of antenna specific Group Delay Variations determined by the Hannover Concept of absolute antenna calibration and the robot of the Institut für Erdmessung (IfE). Group Delay Variations (GDV) may affect the correctness of the position solution in wide area differential GPS applications.**

The paper demonstrates that antenna specific GDV can occur above the code noise level and influences the correctness of the code observation by systematic effects. A detailed study provides strong evidence that code based positioning is improved by up to 0.3 m (or 30%) when GDV are considered. It will be shown if also navigation applications can be improved. Furthermore, we will discuss in detail that GDV do not appear with significant magnitudes on all GPS/GNSS antennas.

Biographies

Tobias Kersten received his diploma in Geodesy from the Technische Universität Berlin in April 2009. Currently he is a research associate at the Institut für Erdmessung (IfE) in the workgroup of Prof. Schön. His research interests are focused on the analyses and studies of absolute antenna calibration with respect to the application of determined corrections for mobile approaches.

Steffen Schön holds a professor-ship in Positioning and Navigation at the Institut für Erdmessung (IfE) since 2006. He has been involved in several GPS projects at DGFI Munich (Germany) and IGMS TU Graz (Austria), especially in the stochastic modelling of errors within GPS processing. The current research interests cover the modelling and correction of systematic errors in GNSS processing like absolute antenna calibration, receiver clock modelling and improved stochastic models for GNSS observations as well as innovative concepts of GNSS navigation.

I. Introduction

For aviation based approaches the study on the code observation including the chain of transmitter - to - receiver is of special interest, since usable signals are restricted and have to be licensed for avionic, sea based and ground based applications like for example curved landing approaches [1], location based ground handling and safety procedures for aircraft [2] as well as sea based landings on aircraft carriers, cf. [3].

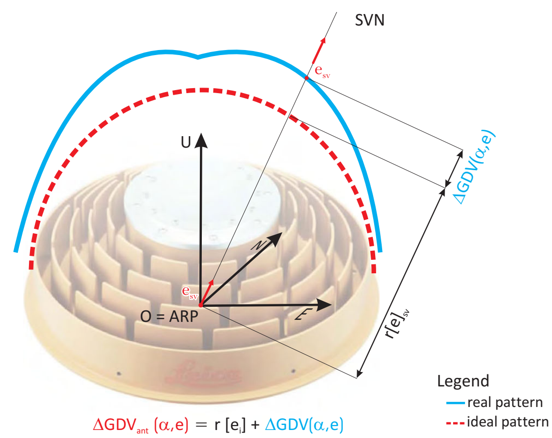

Figure 1: Theoretical concept of GDV expressed in terms of meters and aspect angle of the incoming signal.

Several studies demonstrated that antenna related systematic effects, currently named as group delay variations (code phase variations, GDV) occur for example at Controlled Reception Pattern Antennas (CRPA) [3]. They have to be analysed in detail for the utilization of Global Navigation Satellite Systems (GNSS) for all kinds of navigation approaches. In further analysis, [4] elaborates the importance of and named requirements for the GDV consideration with respect to the Local Area and Wide Area Augmentation Systems (LAAS and WAAS). The precise orbit determination (POD) for low earth orbiters (LEOs) [5] can also be affected, when the GDV impact is above the level of e.g. 0.5 - 1.0 ns.

During studies of the renewal and updating of the Minimal Operational Performance Specifications (MOPS), cf. [6], some GPS antenna show unexpectedly large variations in GDV of some nanoseconds with respect to azimuth and elevation of the incoming satellite signal as examined by [7] and [8], [9].

A GPS antenna is considered as a right-hand circular polarized antenna, cf. [10]. Especially in the electrical engineering the group delay as a measure of the time delay is defined as

$$\delta\tau(\theta,\varphi,f) = \frac{1}{360}\frac{\partial\Phi(\theta,\varphi,f)}{\partial f}, \tag{1}$$

with $\delta\tau(\theta,\varphi,f)$ being the group delay, i.e. the difference of phase φ versus frequency f, and $\Phi(\theta,\varphi,f)$ being the angular part of the phase pattern with the zenith angle θ, cf. [4].

However, in this contribution the GDV are described by the variation w.r.t. the incoming angle of GNSS signal, [9] as also depicted in Figure 1. In theory, the GDV would be zero if the code phase does not change as it is indicated by the dashed line. But in reality the GDV changes with frequency and also with respect to the azimuth α and elevation angle e of the incoming satellite signal; this is indicated by the solid line.

The GDV can be determined using the Hannover Concept of absolute antenna calibration as described by [11]. The extended model, especially for code observations, is described in [12] and [9] by using undifferenced observation and in [13] using a experimental approach with differenced observations. The possible impact on the code observation in the concept of precise code based time and frequency comparison was studied in detail in [14]. We found that the impact of the GDV for this kind of application is definitely below the current code noise level. However, in this contribution we study and discuss the impact of GDV on positioning and navigation.

II. Robot based GDV calibrations

A. Method to determine GDV

First results using the Hannover Concept of absolute antenna calibration to determine elevation dependent Code Phase Variation (GDV) were discussed in [15] and [14] for several geodetic GNSS antennae and receivers.

GDV are obtained during this studies by an extended post-processing method, based on the operational Hannover Concept of absolute antenna calibration, cf. [16], [11]. The set-up is depicted in Figure 2. A 7 m baseline seperates a reference station (MSD8) and a kinematic station (MSD7); both connected to identical receivers (Javad TRE_G3T) with identical firmware and additionally connected to a common external frequency (FS 725 Benchtop Stanford rubidium frequency) supporting one second Allan Variance of $\sigma_y^2 < 2\cdot10^{-11}$. The kinematic station is represented by a precisely calibrated robot arm, that is regularly calibrated at the Geodetic Institute Hannover (GIH) with an accuracy of 0.25 mm, [17]. The robot is used to change the antenna's orientation on subsequent epochs ($<$ 5 seconds) by well known and predefined steps in azimuth as well as elevation.

The antenna calibration is carried out using the actual modulated and available GNSS satellite signals in space. The post-processing of the GDV antenna calibration is based on time differenced single differences.

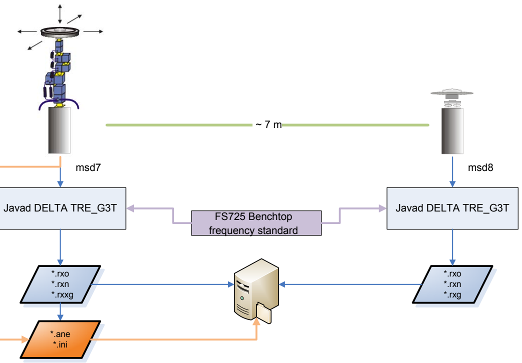

Figure 2: Set-up of antenna calibration based on the Hannover Concept.

B. Observation Model

The code phase observation P_A^j from satellite j to station A is modelled by

$$\begin{aligned} P_A^j &= \rho_A^j + c\cdot(\delta t_A - \delta t^j) + T_A^j + I_A^j + REL_A^j \\ &\quad - d^j + d_A + MP_A^j + GDV_A^j(\alpha,e) + \epsilon_A^j \end{aligned} \tag{2}$$

with the geometric distance ρ_A^j, the synchronization error in meters $c\cdot(\delta t_A - \delta t^j)$ between the system time scale and the receiver clock, the tropospheric T_A^j and ionospheric I_A^j path delay, the relativistic correction REL_A^j, the hardware delays at the satellite d^j and the receiver d_A, multipath effects MP_A^j and possible code phase variations $GDV_A^j(\alpha,e)$ as well as additional observation noise summarized by ϵ_A^j.

Inter-station single differences SD_{AB}^j for each epoch t_ι read

$$\begin{aligned} SD_{AB}^j(t_\iota) &= c\cdot\Delta\delta t_{AB}^j(t_\iota) + \Delta GDV_{AB}^j(\alpha,e,t_\iota) \\ &\quad + \Delta MP_{AB}^j(t_\iota) + \epsilon_{AB}^j(t_\iota), \end{aligned} \tag{3}$$

with the differential receiver clock error $c\cdot\Delta\delta t_{AB}^j$ in meters, the differential GDV of both antennas on the baseline $\Delta GDV_{AB}^j(\alpha,e,t_\iota)$, the differential multipath $\Delta MP_{AB}^j(t_\iota)$, and additional error sources $\epsilon_{AB}^j(t_\iota)$. All satellite specific and distance dependent error sources are eliminated (orbital errors, troposphere and ionosphere) far below the code observation noise level, since they are close similar for both stations.

The $\Delta GDV_{AB}^j(\alpha,e,t_\iota)$ in equation (3) is similar for each epoch since the geometry of visible satellites in the antenna's body frame does not change significantly between two subsequent epochs (maximum delay of less than 5 seconds), so that GDV would be cancelled out on both stations by differentiation of subsequent epochs. Consequently, the orientation of the antenna has to be changed between subsequent epochs by well known and very pre-defined steps in azimuth and elevation which is realized by a robot. The GDV can finally obtained by time differenced single differences on a short baseline with an observation equation that reads

$$\begin{aligned} \Delta SD_{AB}^j(t_\iota,t_{\iota+1}) &= SD_{AB}^j(t_{\iota+1}) - SD_{AB}^j(t_\iota) \\ &= GDV_A^j(\alpha,e) + \epsilon_{AB}^j(t_\iota,t_{\iota+1}). \end{aligned} \tag{4}$$

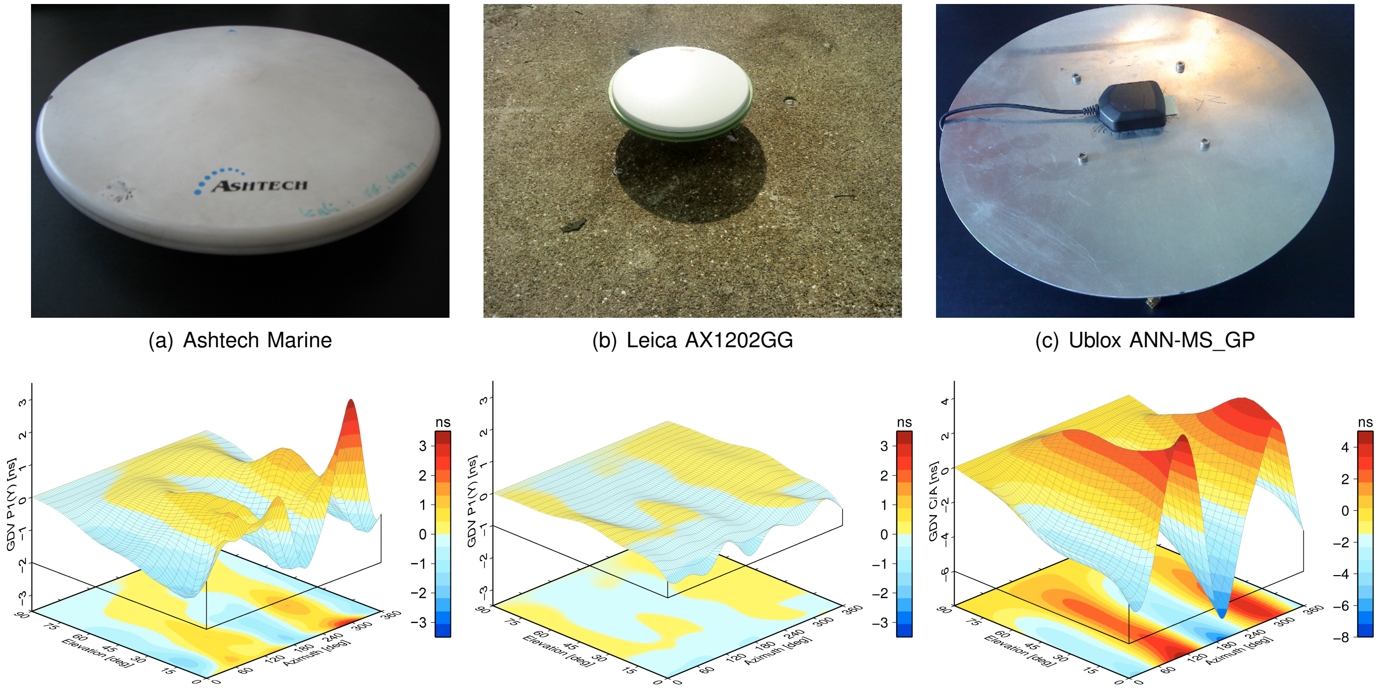

(a) Ashtech Marine (b) Leica AX1202GG (c) Ublox ANN-MS_GP

(d) P1(Y) GDV (e) P1(Y) GDV (f) C/A GDV

Figure 3: Determined GDV for different navigation antennae on GPS P(Y)1 and C/A Signal.

The differential receiver clock error in equation (3) is stable over subsequent epochs and cancels out by differentiation since an external frequency standard is used for both receivers. This is also true for the far field multipath. The impact of the near field multipath is currently analysed at the IfE in a separate study. However, this effect is a challenge at all antenna calibration facilities, chamber as well as robot based approaches.

C. Mathematical Model

GDV are expressed on a sphere by a spherical harmonic analysis

$$GDV(\alpha, e) = \sum_{n=0}^{\infty} \sum_{m=0}^{\infty} \begin{Bmatrix} A_{nm}\, \bar{R}_{nm}(\alpha, e) \\ B_{nm}\, \bar{S}_{nm}(\alpha, e) \end{Bmatrix}, \qquad (5)$$

with unknown coefficients A_{nm} and B_{nm} and

$$\begin{Bmatrix} \bar{R}_{nm}(\alpha, e) \\ \bar{S}_{nm}(\alpha, e) \end{Bmatrix} = \begin{Bmatrix} \cos(m\,\alpha) \\ \sin(m\,\alpha) \end{Bmatrix} N_{nm} P_{nm}(\sin e)$$

with the fully normalized harmonics $\bar{R}_{nm}(\alpha, e)$ and $\bar{S}_{nm}(\alpha, e)$ and a to maximum degree n_{max} and order m_{max} truncated expansion. The harmonics are continuous and orthogonal base functions of elevation e and azimuth α in the antenna's body frame as shown in Figure 1. The normalization factor is denoted by N_{nm} and the associated Legendre functions by $P_{nm}(\sin e)$, as described in [18]. GDV were derived by a best linear unbiased estimator (BLUE) approach (least squares) as shown in [19].

D. Results

Obtained GDV of several GPS antennas were studied and discussed in [15] and [20] among others. To obtain the GDV approx 6000 epochs with up to 22 000 observations were used within a least squares approach using the model (5).

It has to be mentioned that the determined GDV does not depend on the robot sequence during the calibration; this could be shown exemplary by [20] for a calibration of a Ashtech Marine Antenna with different north orientations carried out on different days. In that contribution we have demonstrated, that the obtained pattern was rotated in correspondence to the shifted north orientation of the antenna during the calibration process. In addition, it has to be noted, that GDV only affect the code observation and not the carrier phase. The correction of the phase observation is described by a separate model, named as Phase Center Variations (PCV).

The GDV determination is carried out with a Matlab® based toolbox developed at IfE [21] using the Hannover concept of absolute antenna calibration.

GDV results for antennas used during the experiments in section IV are shown in figure 3 for the P1(Y) signal and the C/A code signal. In the figures 3(a) - 3(c) the calibrated antennas are depicted and in figures 3(d) - 3(f) the obtained GDVs against the elevation and azimuth in a rectangular plot. The antennas have different properties according to the application they are used for. The figures 3(d) - 3(f) express and quantify the antenna specific GDV behaviour. While small variations with an amount of up to 2 ns are illustrated by figures 3(d) and 3(e) with also small azimuthal variations with maximum of 1.0 - 1.5 ns, pronounced GDVs were obtained for the low cost UBlox navigation antenna depicted in figure 3(f).

In the following section we examine the impact of these GDV on the observation and coordinate domain. Additionally, we will demonstrate, that a consideration of GDV will improve the code only based positioning, when antennas with a pronounced and significant GDV pattern are used.

III. Application to static Positioning

A. Observation Domain

The occurring systematic effect was studied by an experiment carried out at the Laboratory IfE rooftop. Therefore, on a short baseline of approx. 7 m two antennas (Leica AR25.R3 LEIT and Ublox) were connected to the identical two receivers (TRE_G3T) which were already used and described during the calibration process. The set-up is depicted in figure 4(a).

Data on C/A was collected on the DOY223-225 in the year 2012 with 30 sec sampling rate and the far field of the experimental set-up was unchanged during the two sidereal repetitions. On DOY223 the antenna on MSD7 was orientated to north (0°) while on DOY224-225 the orientation was changed to 240° by using the same robot as already described in section II.

In order to obtain an idea of the expectable magnitudes of the GDV, the observed minus computed (OMC) inter-station single differences (SD) were analysed in detail. Representative results of an 6 hour observation window for two exemplary satellites are shown in figures 4(b) and 4(c). The OMC is plotted versus time. The elevation of the satellite is indicated by a bright solid line and the GDV along the line-of-sight of the corresponding satellite is indicated by a dark solid line.

The OMC SD of PRN4 shows a noise of up to 0.5 m and a significant trend which does not in corresponds to the ascending and descending satellite (fig. 4(c)). This can be explained by the non-symmetrical behaviour of the UBLOX GDV pattern, cf. figure 3(f). For satellite PRN20 a similar behaviour can be described (fig. 4(c)). It is pretty clear to see, that the trend of the SD OMC for both satellites is described very good by the GDV corrections, plotted as black solid line.

In figures 4(d) and 4(e), the sidereal repeated OMC SD of the same two satellites are depicted. Please note that the difference of the SD OMC are caused by the different north orientation of the Ublox Antenna on MSD7 with a new north orientation of +240°. It can be shown that the systematic effect can be described also very well by the GDV pattern in correspondence to the current antenna orientation.

At this point it can be summarized for the observation domain, that (1) GDV can have a magnitude to degrade the code observations and (2) this effect is repeatable

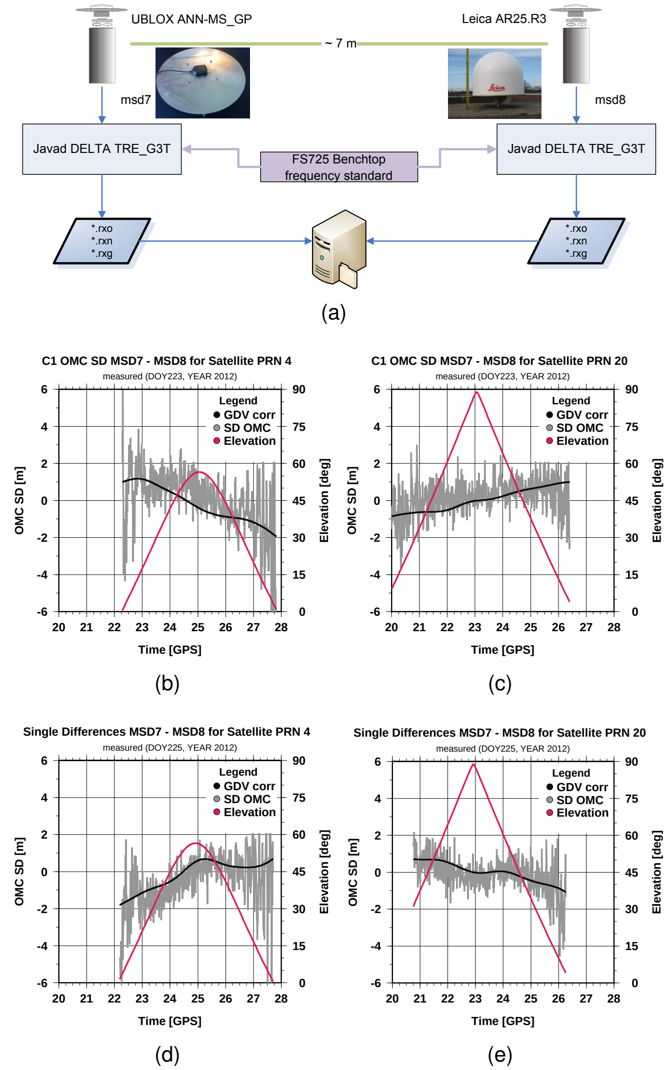

Figure 4: Experimental setup of a short baseline in common clock mode to determine systematics on the C/A observation in a respresentative 6 hour selection.

corresponding to the sidereal repetition of the GPS satellites. Additionally, this effect can be separated from a possible far-field multipath effect, since the latter one would be similar for sidereal repetition and would cause on both days a very similar multipath pattern. But as shown by figures 4(b) - 4(e) this is not the case; a new pattern occurs which must be caused by an additional effect, which depends on the current antenna orientation, i.e. the GDV.

B. Coordinate Domain

As shown for the observation domain, the GDV can also have the magnitude to degrade the code only based autonomous positioning. Therefore, the experimental setup from figure 4(a) was used and autonomous positioning for MSD7 was calculated in several combinations: (1) identical observation-weights [*iden*], (2) elevation dependent weights [*cos*], (3) phase smoothed and

Table 1: RMS of autonomous positioning using a μBlox antenna on the IfE rooftop for 24 hours with 30 Hz data record interval and applying GDV corrections. GPS data was collected on DOY223-225, 2012.

DOY	GDV	RMS of autonomous positioning											
		no phase smoothing						phase smoothing					
		identical weight			elevation weight			identical weight			elevation weight		
		north [m]	east [m]	up [m]	north [m]	east [m]	up [m]	north [m]	east [m]	up [m]	north [m]	east [m]	up [m]
223	no	1.069	0.759	1.972	1.267	0.747	2.354	0.875	0.639	1.798	1.113	0.686	1.891
	yes	0.929	0.697	1.816	1.063	0.717	2.060	0.794	0.572	1.707	0.900	0.645	1.695
		+14%	*+8%*	*+8%*	*+16%*	*+4%*	*+12%*	*+9%*	*+10%*	*+5%*	*+19%*	*+6%*	*+10%*
224	no	0.975	0.733	1.700	0.969	0.705	2.004	0.913	0.648	1.749	0.870	0.649	1.920
	yes	0.862	0.682	1.607	0.971	0.702	1.898	0.738	0.569	1.551	0.874	0.655	1.679
		+12%	*+7%*	*+5%*	*+0%*	*+0%*	*+5%*	*+19%*	*+12%*	*+11%*	*+0%*	*+0%*	*+13%*
225	no	1.093	0.661	2.065	1.104	0.672	2.278	1.097	0.552	2.038	1.000	0.590	2.122
	yes	0.900	0.625	1.742	1.038	0.646	2.057	0.800	0.494	1.680	0.904	0.574	1.814
		+17%	*+0%*	*+15%*	*+6%*	*+4%*	*+10%*	*+27%*	*+11%*	*+18%*	*+10%*	*+3%*	*+15%*

identical weights [*sm iden*] and (4) phase smoothed and elevation dependent weights [*sm cos*].

The observation equation (2) was used to calculate an epoch-wise single point positioning (SPP) as described in [22] which reads

$$\Delta\mathbf{l} + \mathbf{v} = \mathbf{A}\Delta\mathbf{x}, \tag{6}$$

were $\Delta\mathbf{l}$ is the (n×1) vector containing the OMC (i.e. the difference of computed $\mathbf{P_c}$ and measured $\mathbf{P_m}$ pseudoranges)

$$\begin{aligned}
\Delta\mathbf{l} &= \begin{bmatrix} P_m^{(1)} - PR_c^{(1)} \\ \vdots \\ P_m^{(n)} - P_c^{(n)} \end{bmatrix}, \\
P_c^{(j)} &= \rho_A^j + c\cdot\delta t_A^j + T_A^j + I_A^j + GDV(\alpha, e)_A^j,
\end{aligned}$$

$\mathbf{v}$ is the (n×1) residual vector, $\mathbf{A}$ is the (n×4) design matrix per epoch t_ι,

$$\mathbf{A} = \begin{bmatrix} -\frac{\Delta X_A^{j^{(1)}}}{\rho_A^j} & -\frac{\Delta Y_A^{j^{(1)}}}{\rho_A^j} & -\frac{\Delta Z^{j^{(1)}}}{\rho_A^j} & 1 \\ \vdots & \vdots & \vdots & \vdots \\ -\frac{\Delta X_A^{j^{(n)}}}{\rho_A^j} & -\frac{\Delta Y_A^{j^{(n)}}}{\rho_A^j} & -\frac{\Delta Z_A^{j^{(n)}}}{\rho_A^j} & 1 \end{bmatrix}$$

with the coordinate difference $\Delta X_A^{j^{(n)}}$ between the satellite j and the ground station A at epoch t_ι; $\Delta\mathbf{x}$ is the (4×1) unknown vector and n the number of satellites at every epoch. The ionospheric delay is corrected by the Klobuchar model [23] and the tropospheric correction is considered by applying the Hopfield model, [24].

Finally, the estimated unknowns are obtained by

$$\Delta\mathbf{x} = (\mathbf{A^T P A})^{-1}\mathbf{A^T P}\boldsymbol{\Delta}\mathbf{l}, \tag{7}$$

with the $(n\times n)$ matrix $\mathbf{P}$ of weights with diagonal elements

$$\begin{aligned}
p_{ii} &= 1 \quad \text{(identical weighting) or} \\
p_{ii} &= \sin^2(e) \quad \text{(elevation weighting)}
\end{aligned}$$

with the elevation angle e of the respective incoming satellite signal.

The smoothing of code observations was carried out by combining 25 epochs of phase pseudoranges with the corresponding code observations and a cut off angle of 5°.

The coordinates residuals are obtained by comparing the SPP determined coordinates against coordinates from a precise 3d static measurement set-up with carrier phase observations. The results of all combinations are summarized in table 1. It can be seen that the consideration of GDV corrections does improve the SPP solution at any time, although most benefit is obtained by using phase-smoothed code observations. Improvements of approx 0.1 - 0.2 m (+10%) in the north component and up to 0.2 - 0.3 m (+15%) in the up component can be identified. Some smaller improvements exists for the east component. This is pretty clear since for phase smoothed observations , the code noise could be reduced and they can be improved by the GDV corrections. Applying the elevation dependent weighting to the observations leads to less improvement of the GDV corrections. This is explainable by the very pronounced GDV pattern of the Ublox antenna at low elevations, cf. figure 3(f). This means, without GDV corrections, a elevation weighting can already reduce the GDV impact on the code-only solution. This is only valid and meaningful, if the GDV pattern is well pronounced in azimuth and elevation and shows magnitudes over the level of significance, i.e. above th code observation noise of approx. 0.3 -1.0 m. As shown in [13] this is not valid for all antennas.

For a detailed analysis of the improvement of the SPP derived coordinates, in figures 5(a) - 5(c) we present coordinate time-series with sidereal repetition for the DOY223-225, with and without considering GDV corrections.

From figure 5(a) it can be clearly seen that the north and up component can be improved significantly in contrast to the east component, which stays nearly the same.

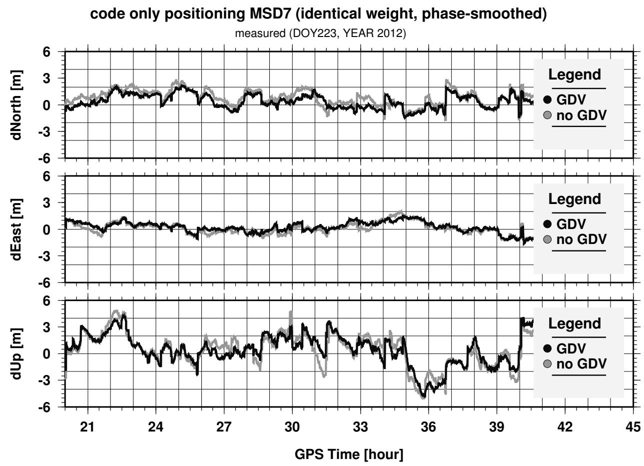

(a)

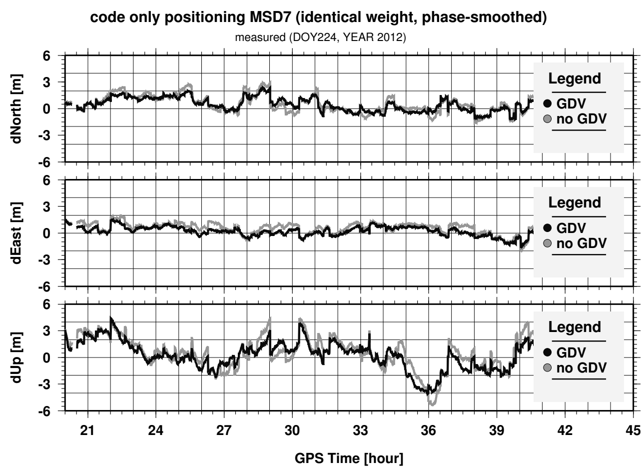

(b)

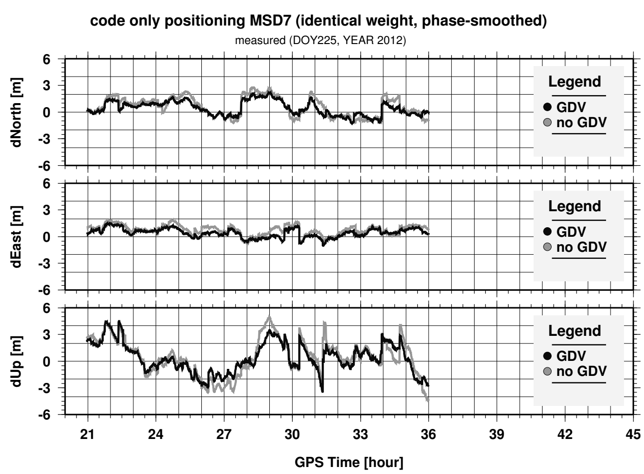

(c)

Figure 5: Static positioning improved by applying GDV corrections to observables.

Improvements of up to 1.5 - 2.0 m (up component) are achievable. This behaviour is also valid for the sidereal repetition of the coordinate time series, cf. figures 5(b) and 5(c).

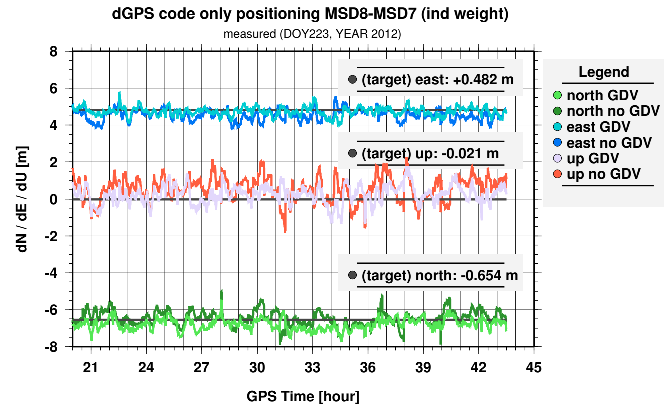

(a)

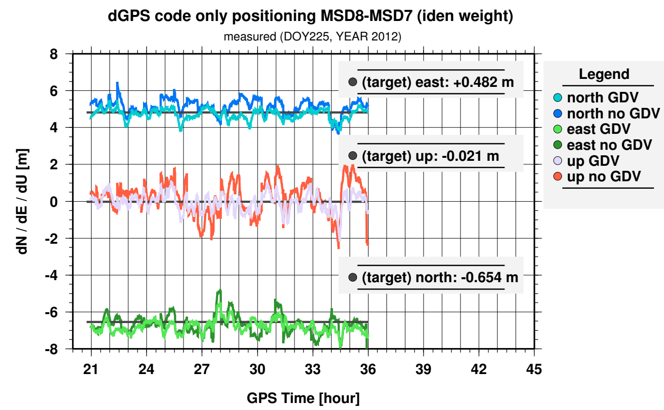

(b)

Figure 6: Improvement of the code based relative positioning is demonstrated by considering GDV corrections on a short 7 m baseline. the reference value is given for each coordinate component.

Table 2: RMS of small Baseline MSD7-MSD8 using a Leica AR25 as reference and a μBlox Antenna as rover on the IfE rooftop for 24 hours with 30 sec sampling interval and with/without GDV consideration.

DOY	GDV	RMS of Baseline MSD8-MSD7 (code only, iden. weigth) no phase smoothing			phase smoothing		
		north [m]	east [m]	up [m]	north [m]	east [m]	up [m]
223	no	0.864	0.623	1.355	0.476	0.295	0.728
	yes	0.789	0.597	1.277	0.362	0.238	0.560
		+8%	+4%	+6%	+23%	+19%	+23%
225	no	0.953	0.634	1.519	0.679	0.397	1.008
	yes	0.794	0.574	1.259	0.438	0.292	0.545
		+16%	+9%	+17%	+35%	+26%	+45%

Furthermore, improvements for the code based relative positioning are expectable in the case of very different and pronounced GDV patterns. This is depicted in figures 6(a) and 6(b) as well as additionally in table 2 for two days in sidereal repetition. To obtain the relative positioning, inter-station SD of station MSD7 and MSD8 of the IfE rooftop were introduced in the navigation algorithm (6). The components of the baseline show an improvement of up to 0.17 m but now for all three components, although the up component benefits mostly. It is demonstrated that variations during the 24 hour time span are significantly reduced by considering the GDV corrections and that this improvement is also repeatable on sidereal repetition and changed antenna orientation.

IV. Application to kinematic positioning

A. Method

The GDV were verified within a practical automotive navigation approach where three different antennas (already described in section II-D) mounted on a car rooftop were used to collect data for three trajectories instantaneously in one round, cf. figure 7, whereby 4 independent runs were performed. Trajectories were driven on a test area in Ahlten, Hannover, which provides very good conditions like a wide flat field and a very good satellite visibility. As shown in figure 7(d) one complete turn goes from start to part1 to part 2 and so on until the it is closed at the starting point. Measurements were obtained on DOY037, 2013.

To keep the GDV corrections consistent with the current navigation frame of the mobile platform, a computer controlled navigation system (CCNS) from IGI with an IMU and a GPS Receiver (Ashtec Z12 II) was used to precisely determine the position, velocity and attitude of the sensor. The CCNS4 unit runs with a sampling rate of 64 Hz, whereby the receivers connected to the antennas under test were operated at 10 Hz. The navigation azimuth were obtained by post-processing using IGI Aero Office Software package; an external GPS solution was calculated with GrafNav Waypoint Software in differential GPS with phase information.

B. GDV impact on trajectories in observation domain

The azimuth α_A^j of the incoming satellite signal of satellite j in the topo-centric antenna coordinate system of antenna A has to be corrected w.r.t the current orientation α_{nav} of the mobile platform. Therefore the azimuths were corrected by the navigation azimuth like

$$\alpha_{A,corr}^j = \alpha_A^j - \alpha_{nav}$$

and GDV corrections ($GDV_A^j(\alpha_{corr}, e)$) w.r.t. the trajectory can be computed and applied to the observations.

In Figure 8 the yaw angle and the corrected satellite azimuth are depicted versus the corresponding GDV correction along the line of sight for the μBlox antenna. It can be demonstrated that at high elevations small variations of below 0.3 m can be expected as shown in figure 8(a), whereby at low elevations the corrections can induce magnitudes of up to 3 m (cf. 8(b)), which is definitely related to the antenna specific GDV, cf. figure 3(f), too. Rather sudden jumps of 3 m are induced by the ad-hoc changes of the orientation. These changes occur, as soon as the mobile platform was moved by up to 90 degrees in azimuth. Since the GDV pattern of the μBlox antenna is very symmetric, one moves at low elevation from one minimum to a maximum or vice versa.

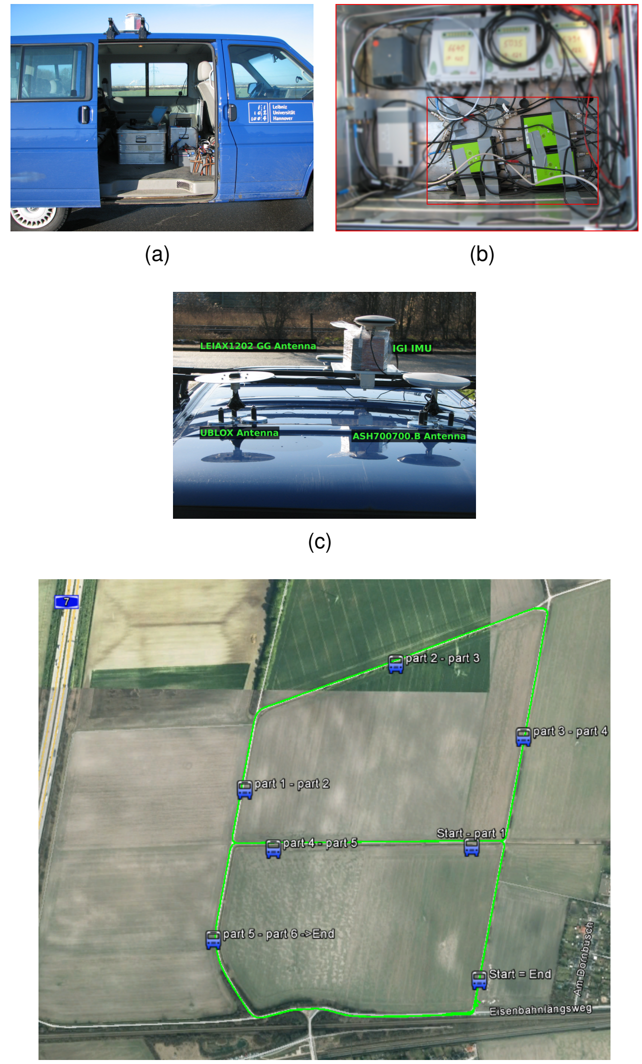

Figure 7: Instrumentation used to collect the GPS trajectories (a), with different receivers (b) connected to three antennae (c) on a test area in Ahlten (City of Lehrte) to obtain GPS trajectories for different navigation antennas simultaneously (d).

As long as no code-phase smoothing is applied to the observations, one can detect small jumps near below the level of significance. The effect can completely removed form the raw observations if an appropriate code-phase smoothing is applied. However, in this paper the validation is performed on the coordinate domain with identical weighting to obtain access to the GDV related impact, so the reader will kindly refer to the last subsection.

C. GDV impact on trajectories in position domain

The trajectories are validated using a Matlab® software toolbox developed at IfE. During the validation in a epoch-wise code single point positioning (SPP) algorithm, several processing schemes (equal and elevation dependent weighting, code-phase smoothing, different cutoff angles) were calculated to cross-check the solutions and to store the corresponding statements.

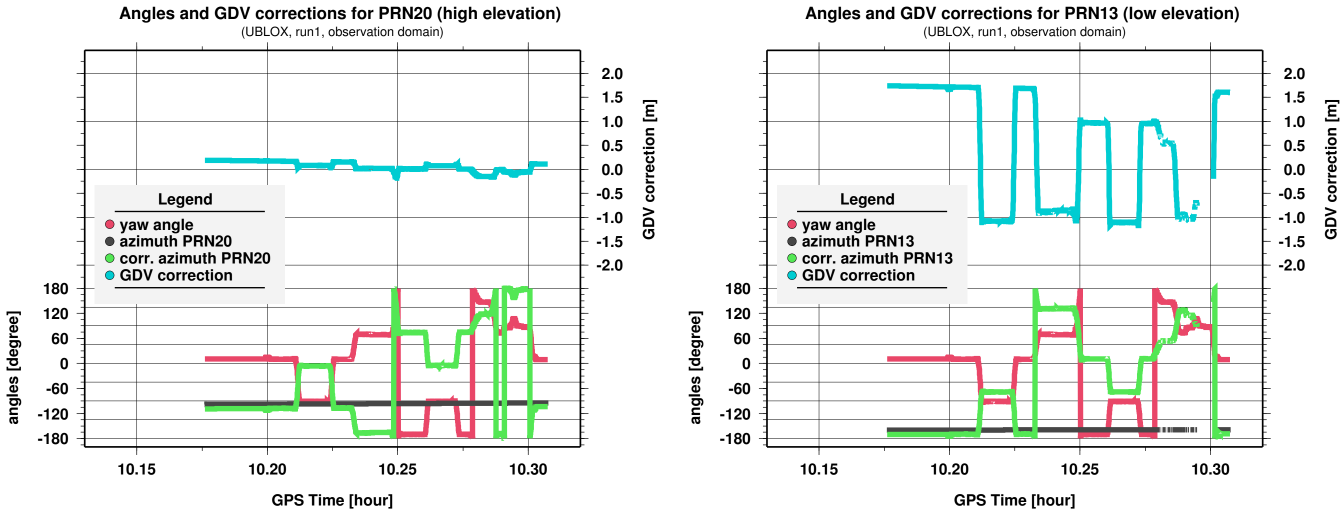

(a) corrections for μBlox antenna

(b) corrections for μBlox antenna

Figure 8: Individual satellite azimuth and yaw angles versus GDV correction as shown for satellite with high (a) and low (b) elevation.

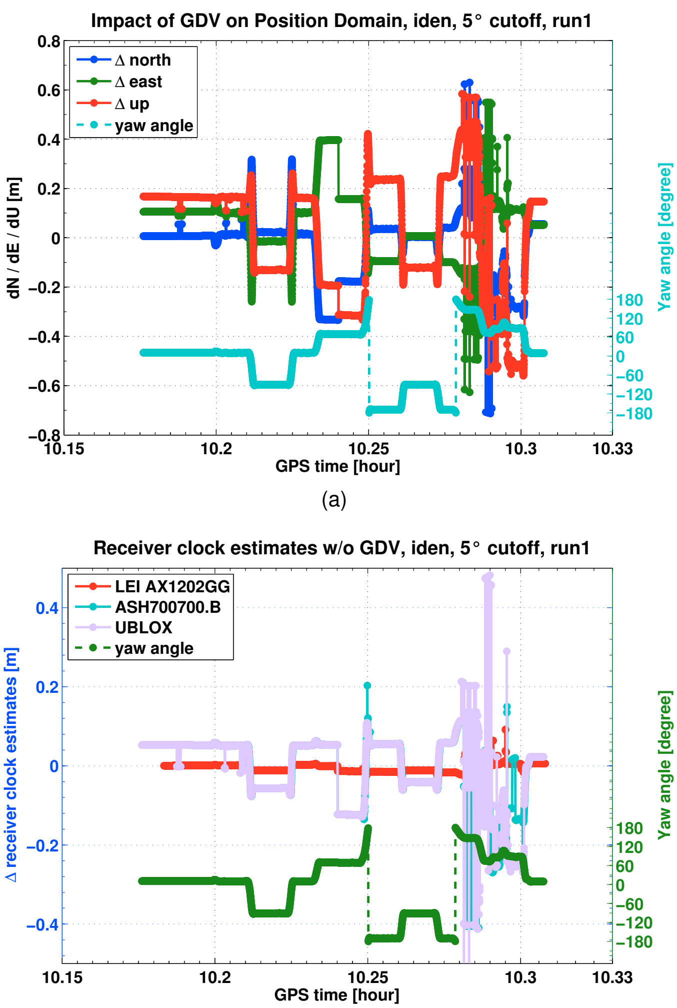

Figure 9: Impact of GDV on the position domain and on the receiver clock estimates for μBlox antenna, run1.

From the cross check and the study of the validation we can summarize that the GDV impact on the observation domain is very small for all of our 3 antennas tested. Any usage of elevation weighting and or code-phase smoothing reduce this effect below the code noise. This is especially true for antennas already showing small magnitudes in GDV and their corresponding GDV correction. Since pronounced GDV pattern is expectable at low elevations an elevation weighting will also reduce the impact. Therefore, our studies were focussed on the combination of non smoothed pseudo-ranges, identical weighting and a cutoff angle of 5 degree.

To obtain the impact of the GDV correction on the position domain, both trajectories (with and without GDV correction) were compared to each other. In figure 9(a) differences for the μBlox antenna versus the yaw angle, obtained from the first run are shown. The sudden jumps of the topocenter coordinate components are again due to the orientation changes of the platform, as also shown in the observation domain. However, the magnitudes of the jumps are in the order of 0.2 - 0.6 m, quite below the code noise. For example, the up component is influenced by a jump of 0.3 m for a 90° turn in azimuth, cf. figure 9. The corresponding north and east component are influenced in the same way, since the pattern of the μBlox antenna is very pronounced. However, applying a simple SPP algorithm some smaller variations of the GDV impact is also collected in the receiver clock estimates. Referring to figure 9(b) this effect is shown for the receiver clock estimates of run 1 and for all three trajectories. The pronounced impact can be detected for the μBlox and the Ashtech ASH700700.B antenna whereby for the Leica LEIAX1202GG these variations are at the level of insignificance.

To summarize, GDV neither improve nor degrade the SPP derived epochs-wise navigation of mobile platforms. But it has to pointed out that for this approach the internal

Table 3: Comparison of individual trajectories with respect to the corresponding external GPS solutions, obtained with GrafNav Waypoint.

RMS of trajectories w.r.t. external solution					
run	**antenna**	GDV	north [m]	east [m]	up [m]
1	μBLOX	yes	1.523	1.277	1.684
		no	1.154	1.280	1.673
	Leica AX1202GG	yes	1.159	1.225	1.495
		no	1.150	1.222	1.496
	Ashtech ASH700700.B	yes	0.686	0.926	0.881
		no	0.663	0.939	0.915
4	μBLOX	yes	0.939	1.046	1.783
		no	0.919	1.044	1.737
	Leica AX1202GG	yes	1.000	1.245	0.957
		no	1.001	1.253	0.954
	Ashtech ASH700700.B	yes	0.512	0.424	0.819
		no	0.533	0.451	0.810

receiver clocks were used, whereby an external receiver clock with a improved frequency stability was used during the experiments described in section III, although the same SPP algorithm was used. The behaviour of the individual receiver clocks used in the navigation approach could lead to a poorer estimation. In the same way we have demonstrated, that the impact of GDV, although pronounced, is below the precision of the receiver clock estimation. Therefore the GDV have no impact on the code only solution. In a further step during the analysis of the individual trajectories differences to a nominal solution were calculated and some results are exemplarily shown in table 3 were the RMS of the differences are shown. The solutions demonstrate, that there is no significant and systematic effect.

V. Conclusion

In this contribution we have demonstrated that GDV exists for GPS/GNSS antennas and that some antennas show pronounced GDV patterns. Furthermore we have described a calibration concept for obtaining the antenna specific GDVs using the Hannover concept of absolute antenna calibration in combination with an experimental GDV post processor.

It has to be mentioned, that the determined GDV are not only a function of the antenna but also of the used receiver (tracking properties) and cable accessories, too. In that way, GDV are only valid for the specific combination of the elements, since the GDV is a time delay measurement. Therefore, it was important, that the same receivers were used for the evaluation of the GDV on the observation and coordinate domain. Standard tracking parameters were used for the calibration and the performed experiments. Additionally, we have also discussed that GDV are independent of the orientation of the antenna during the calibration, cf. [13].

In the case of static positioning it was demonstrated that GDV can influence not only the precision but also the correctness of the code observation. Improvements of +10% (10-20 cm for the north component and up to 30 cm in the up component) and even more for phase-smoothed observations are obtained. It could also be shown by different antenna orientation that the systematic effects on the OMC SD observations are pretty well described by the determined GDV pattern and not by a possible multipath effects. Furthermore, improvements in the coordinate domain of up to 8% (up to 11% when code smoothing is applyied) are obtainable. In addition it was elaborated that relative code positioning also benefits form the GDV consideration.

In a navigation approach we have validated the impact of GDV on code only solutions for several antennas. The individual and antenna specific GDV were applied and compared to (1) the same trajectory with and without GDV and (2) against a nominal, external DGPS solution, to estimate the impact on the position domain. During the studies it could be evaluated that elevation dependent weighting does also reduce a possible GDV effect since the pronounced GDV magnitudes can be expected at low elevation.

To bring the paper to a close we summarize that the GDV does not have significant impacts on our navigation scenario. This could be quantified by comparing the impact on the coordinate domain, which provides magnitudes of up to 0.2 - 0.3 m well below the level of significance. We have also demonstrated that the GDV effect is collected in the receiver clock estimates with maximum magnitudes of 0.2 m, when a simple code based and epoch-wise SPP algorithm is used. One possible reason is the usage of individual receiver clocks during the data collection of the kinematic trajectory, while for static experiments in section III we used a common clock with a stable frequency stability for both receivers. Indeed the GDV will have a larger impact when a very stable clock in combination with an antenna which provides pronounced GDV is used, but this does not reflect the reality in most of cases. However, this idea this not entirely absurd since chip scaled atomic clocks (CSAC) and similar products have found an enhanced way onto the market and are more and more used for navigation approaches. Further studies focussing the quality of CSAC were analysed for static and kinamatic cases at IfE. Currently GDV are not a significant source of error and limiting factor so far, but it could be if the code noise of the raw observation will be reduced, which is the fact for the new Galileo signals E5a/b, in combination with the usage of precise and stable clocks.

Disclaimer

Although the authors dispense with endorsement of any of the products used within this study, commercial products were named for scientific transparency. Please note that a different receiver / antenna unit of the same manufacturer and type may show different characteristics.

Acknowledgment

The work in this project is supported by the German Aerospace Centre (DLR), funded by the Federal Ministry of Economics and Technology (BMWI), based on a resolution of the German Bundestag.

The authors grateful acknowledge the Landesamt für Geoinformation und Landentwicklung Niedersachsen (LGLN) for supporting reference station data for our differential GPS solution. Furthermore we would like to thank Thomas Krawinkel for his assistance during the practical experiment.

REFERENCES

[1] F. Kube, S. Schön, and T. Feuerle, "GNSS-based Curved Landing Approaches with a Virtual Receiver," in *Proceedings of the Position Location and Navigation Symposium (ION-PLANS), 2012 IEEE/ION*, 23-26. April, Marriott Resort & Spa, Myrtle Beach, South Carolina 2012, pp. 188 – 196.

[2] G. Pastana, A. Kutvonen, A. Kurz, and A. Casaca, "Location-based Services to Improve Aircraft Ground Handling and Safety Procedures," *European Journal of Navigation*, vol. 8, no. 3, pp. 16–21, 2010.

[3] K. U. Suok, "Analysis of Carrier Phase and Group Delay Biases Introduced by CRPA Hardware," in *Proceedings of the 18th International Technical Meeting of the Satellite Division of The Institute of Navigation (ION GNSS 2005)*, 13 - 16. September, Long Beach, CA 2005, pp. 635–642.

[4] F. van Graas, C. Bartone, and T. Arthur, "GPS Antenna Phase and Group Delay Corrections," in *Proceedings of the 2004 National Technical Meeting of The Institute of Navigation*, 26-28. January, San Diego, California, USA 2004, pp. 399–408.

[5] O. Montenbruck, M. Garcia-Fernandez, Y. Yoon, S. Schön, and A. Jäggi, "Antenna Phase Center Calibration for precise position of LEO Satellites," *GPS Solut*, vol. 13(1), pp. 23–34, 2009.

[6] RTCA, "Minimum Operational Performance Standards for Global Navigation Satellite System (GNSS) Airborne Active Antenna Equipment for the L1 Frequency Band," *RTCA/DO-301*, 2006, inc. Washington DC, Issued: 12/13/2006.

[7] W. Kunysz, "Effect of Antenna Performance on the GPS Signal Accuracy," in *Proceedings of the 1998 National Technical Meeting of The Institute of Navigation (NTM 98)*, 21. - 23. Januar, Westin Long Beach Hotel, Long Beach, California USA 1998, pp. 575–580.

[8] T. Murphy, P. Geren, and T. Pankaskie, "GPS Antenna Group Delay Variation Induced Errors in a GNSS Based Precision Approach and Landing Systems," in *Proceedings of the 20th International Technical Meeting of the Satellite Division of The Institute of Navigation (ION GNSS 2007)*, 25.-28. September 2007, Fort Worth Convention Center, Fort Worth, Texas, USA 2007, pp. 2974 – 2989.

[9] B. R. Rao, W. Kunysz, R. L. Fante, and K. McDonals, *GPS/GNSS Antennas*. Artech House Publishers, Norwood, USA, 2013.

[10] IEEE Standards, "IEEE Standard Test Procedures for Antennas," *ANSI/IEEE Std 149-1979*, p. 135, 2008. [Online]. Available: http://ieeexplore.ieee.org/xpl/articleDetails.jsp?arnumber=19510

[11] G. Wübbena, M. Schmitz, F. Menge, V. Böder, and G. Seeber, "Automated Absolute Field Calibration of GPS Antennas in Real-Time," *ION GPS 2000*, pp. 2512–2522, 2000.

[12] G. Wübbena, M. Schmitz, and M. Propp, "Antenna Group Delay Calibration with the Geo++ Robot - extensions to code observable," in *IGS Analysis Workshop, Poster, June 2-6 Miami Beach Florida, USA*, 2008.

[13] T. Kersten and S. Schön, "Antenna specific IfE-Robot based Code Phase Delays and its Impact on Positioning and Navigation," in *6th ESA Workshop on Satellite Navigation Technologies and European Workshop on GNSS Signals and Signal Processing (NAVITEC), 5.-7. December, ESTEC, Noordwijk, The Netherlands*, 2012, p. 8.

[14] T. Kersten, S. Schön, and U. Weinbach, "On the Impact of Group Delay Variations on GNSS Time and Frequency Transfer," in *Proceedings of the 26th European Frequency and Time Forum (EFTF)*, 24.-26. April 2012, Göteborg, Sweden 2012, pp. 1–8, in press.

[15] M. Schmitz, G. Wübbena, and M. Propp, "Absolute Robot-Based GNSS Antenna Calibration - Features and Findings," in *International Symposium on GNSS Space-Based and Ground-Based Augmentation Systems and Applications*, Berlin, Germany, November 11. - 14. 2008.

[16] V. Böder, F. Menge, G. Seeber, G. Wübbena, and M. Schmitz, "How to Deal With Station Dependent Errors - New Developments of the Absolute Field Calibration of PCV and Phase-Multipath With a Precise Robot," in *14th International Technical Meeting of Satellite Division of the U.S. Institute of Navigation (ION GPS 2001)*, 11.-14. September, Salt Lake City, Utha USA 2001, pp. 2166–2176.

[17] V. Meiser, "Kalibrierung des GNSS-Antennenkalibrierroboters des Institut für Erdmessung mittels Lasertracking," Geodätisches Institut Hannover (GIH), Leibniz Universität Hannover, Tech. Rep., September 2009.

[18] Hobson, *The Theory of spherical and ellipsoidal Harmonics*. Cambridge, University Press, 1931.

[19] T. Kersten and S. Schön, "On the Determination of Antenna Phase Center Corrections in a Multi-GNSS Multi-Frequency Approach," in *EGU General Assembly 2011*, ser. Geophysical Research Abstracts, #EGU2011-3678, vol. 13, no. EGU2011-3678, 03. - 08. April 2011 2011, Poster.

[20] ——, "Current Research Activities at the IfE Antenna Calibration Facility," in *IGS Workshop 2012*, Olsztyn, Poland, July 23-27 2012, Poster.

[21] ——, "ACA_IfE - Ein Matlab Post-Prozessor zur Bestimmung von Antennenspezifischen GPS Code-Phasen Variationen (GDV)," in *Entwicklerforum Geodäsie und Geoinformationstechnik*. Institut für Geodäsie und Geoinformationstechnik (IGG), Technische Universität Berlin, 27.-28. September 2012, p. 9, in press.

[22] G. Seeber, *Satellite Geodesy*. Walter de Gruyter, 2003.

[23] J. Klobuchar, "Ionospheric time-delay algorithm for single-frequency gps users," *IEEE Transactions on Aerospace and Electronic Systems*, vol. AES-23, no. 3, pp. 325–331, 1987.

[24] H. S. Hopfield, "Two-quartic tropospheric refractivity profile for correcting satellite data," *Journal of Geophysical Research*, vol. 74, no. 18, pp. 4487–4499, 1969.